



A Sustainable Approach for the Synthesis of Poly(3-hydroxybutyrate-co-3-hydroxyvalerate) Biocomposite by Employing Corncob-Derived Nanocellulose as a Reinforcing Agent

Sanjana Narayanan¹ · Sameena Anjum¹ · Angana Chaudhuri¹ · P. Radha¹

Accepted: 26 November 2020 / Published online: 5 January 2021

© The Author(s), under exclusive licence to Springer Science+Business Media, LLC part of Springer Nature 2021

Abstract

Poly(3-hydroxybutyrate-co-3-hydroxyvalerate) (PHBV) is a copolymer synthesized by *Bacillus megaterium* co-utilizing cheese whey and food waste hydrolysate for its one-step production. The optimized substrate ratio of 60:40 (v/v) manifested maximum biomass of 3.09 ± 0.12 g/L and PHBV yield of 2.0 ± 0.3 g/L. Batch kinetics study revealed maximum biomass and PHBV yield of 3.05 ± 0.07 g/L and 2.175 ± 0.06 g/L respectively, with $71.43 \pm 0.28\%$ g/g PHBV content. The integration of corncob-derived nanocellulose into PHBV was confirmed by scanning electron microscopy (SEM), Fourier transform infrared spectroscopy (FT-IR), and X-ray diffraction (XRD) analysis. Thermogravimetric analysis (TGA) and differential scanning calorimetry (DSC) analyzed the thermal characteristics of the PHBV biocomposite, where the highest degradation temperature was obtained at 790 °C, thus exhibiting high thermal stability. The mechanical properties such as Young's modulus, elongation at break, and tensile strength of the biocomposite was comparatively higher than PHBV and was found to be 40 MPa, 5.310%, and 11.110 MPa, respectively. The enhanced thermal and mechanical characteristics of PHBV biocomposite proves that the corncob-derived nanocellulose can be employed as a reinforcing agent.

Keywords PHBV · *Bacillus megaterium* · Cheese whey · Food waste hydrolysate · Corncob-derived nanocellulose · PHBV biocomposite

Introduction

In recent years, the synthetic plastic wastes, the non-biodegradable plastic micro-particles, and the production of toxic substances during its degradation have raised serious environmental concerns. Moreover, the availability of oil resources for manufacturing synthetic plastics have dropped remarkably with a rise in worldwide demand. Biopolymers' emerging development is a promising approach and an environmentally benign alternative to synthetic plastic due to its biodegradability and lowered toxicity [1]. The most promising and sustainable substitute for synthetic plastics is polyhydroxyalkanoate (PHA), a family of naturally

biodegradable intracellularly produced polyesters reserved as energy by different bacteria [2]. The production of PHA from renewable carbon sources has made the use of polyesters environment-friendly [3]. Poly(3-hydroxybutyrate-co-3-hydroxyvalerate) (PHBV), a very promising bio-sourced and biodegradable bacterial copolymer with two monomeric units of 3-hydroxybutyrate (3HB) and 3-hydroxyvalerate (3HV) [4]. *Bacillus megaterium*, a saprophytic, endospore-forming, aerobic bacteria, has gained importance in biotechnology due to its ability to produce polymers [5]. The organism has its unique ability to utilize excess carbon source for synthesizing PHA, which further includes 3-, 4-, 5- and 6-hydroxyl acid monomers [6]. These properties of *B. megaterium* can be exploited to make it an excellent source for the biological synthesis of PHBV.

The carbon sources for the production of PHBV account for almost 50% of the total estimated cost [7]. Cheese whey is one of the most abundantly found by-products in the dairy industry and represents 70–80% of the volume of transformed milk. The cheese whey contains about 50% of the original milk's nutrients and has high lactose quantity

✉ P. Radha
radhap@srmist.edu.in

¹ Bioprocess and Bioseparation Laboratory, Department of Biotechnology, School of Bioengineering, College of Engineering and Technology, SRM Institute of Science and Technology, Kattankulathur, Kanchipuram District, Tamil Nadu 603203, India

[8]. The high amount of lactose in the cheese whey can be suitably used as a carbon source for the production of 3HB monomeric units, which are used for polymerizing poly(3-hydroxybutyrate) [9]. In general, synthetic plasticizers are co-fed as media components to induce the formation of 3HV monomeric units, leading to the production of PHBV, a condensation polymer of hydroxybutyric acid and hydroxyvaleric acid [10]. Hence, volatile fatty acids (VFAs) such as propionic acid, butyric acid, and valeric acid, derived from anaerobic digestion (AD) of various industrial wastes, can replace the use of synthetic plasticizers for the synthesis of PHBV, thus serving the benefit of waste management and cost-effective production.

Food waste proves to be a suitable raw material for the AD, which can produce biogas and VFAs. In recent days, the recovery of various acids from food waste through AD has attained much attention [11]. The rich nutrients and appropriate moisture content of food waste make it ideal for the digestion. VFAs such as butyrate, acetate, propionate, and valerate is synthesized in the first three phases of AD [11]. These are regarded as commercially valuable chemicals. The intermediate VFAs prove to influence the content of 3HB and 3HV due to its availability and composition [12]. The VFAs produced are ideally suitable for PHBV production [13]. Valerate or valeric acid present in the food waste hydrolysate act as the precursor for 3HV units. The 3HB and 3HV monomeric units together form PHBV [14]. Previous studies reported that the addition of propionic acid or other VFAs along with cheese whey in the medium elevated the PHBV yield than utilizing cheese whey or VFA solely for PHBV production [10, 12, 13]. Moreover, food waste hydrolysate acts as the primary source for VFAs; thus, combined utilization of food waste hydrolysate and cheese whey enhances the production of PHBV.

One of the natural fibers present in plants with exceptional mechanical properties, biodegradable, non-toxic, and renewable, is cellulose [15]. It has an extensive application in the field of biopolymers. Cellulose comprises linear polymers with hydroxyl groups attached to it, responsible for the strong bonding [16]. In some of the recent studies regarding the usage of waste oil palm empty fruit bunch fiber [17], coffee silverskin [18], almond shell flour [19], vine shoots [1], sugarcane bagasse [20], wheat husk [21], olive pomace fibers [4], groundnut shell [22] and winery waste [23], has portrayed them as reinforcing agents in the polymeric matrices and as a promising value-added agro-wastes. Corncob being a cheap and globally available agricultural residue, primarily comprises cellulose, which in the nanoscale can be reinforced in the polymers to form polymer biocomposites [24]. Given the high availability of cellulose across agricultural sectors, it is an excellent sustainable and renewable source [25–28].

Different techniques have been used to synthesize nanocellulose, such as acid hydrolysis, mechanical methods, and enzymatic hydrolysis [29–31]. Acid hydrolysis is widely used, as this method is easy and fast to produce nanocellulose with better properties. The employment of acids to catalyze the hydrolysis of hemicellulose and cellulose is a very beneficial method [32]. The crystallinity of the nanocellulose derived from acid hydrolysis was comparatively higher [33]. Further, the acid hydrolysate can be mechanically treated to convert cellulose into nano form [34]. This nanocellulose imparts unique characteristics such as low density, biodegradability, and good mechanical properties. Moreover, incorporating the nanocellulose in the range of 1–15 wt% in PHBV, termed as PHBV biocomposites, causes a notable enhancement in the thermal and mechanical stability, making it an ideal bio-based reinforcing agent [35–37]. Thus, the PHBV biocomposites have been regarded as a promising alternative to conventional polymers as they serve to diminish environmental pollution, greenhouse gas emissions, and depletion of fossil fuels [38].

To the best of our knowledge, PHBV has never been synthesized by co-utilizing cheese whey and food waste hydrolysate, and further integrated with corncob-derived nanocellulose to produce PHBV biocomposite, thus, proving it as a novel and unconventional idea. Further, the physical and chemical characterization of the PHBV biocomposite were analyzed by various analytical techniques such as gas chromatography-mass spectrometry (GC–MS), Fourier transforms infrared spectroscopy (FT-IR), scanning electron microscopy (SEM), transmission electron microscopy (TEM), and X-ray diffraction (XRD) analysis. Moreover, the thermal and mechanical properties such as thermogravimetric analysis (TGA), differential scanning calorimetry (DSC), tensile strength, Young's modulus, and elongation at break were studied for its suitability in various applications. Biodegradability analysis was performed to examine the degradability nature of the biocomposite.

Materials and Methods

Materials

Bacillus megaterium NCIM 5472 was purchased from National Centre for Industrial Microorganisms, Pune, India. The nutrient agar medium for the growth of *B. megaterium* comprises components, as mentioned by Bhattacharya et al. [39] and preserved at 4°C. Further, cheese whey complemented with minimal salts media and trace elements was used as production media. Food waste for VFA production was procured from campus mess. Corncob waste residue was collected from local market disposals.

Volatile Fatty Acid (VFA) Production

The food waste collected from the campus mess, comprising mainly rice, cereals, vegetables, and bread, was anaerobically digested to produce VFAs. The food waste was pulverized and transferred to digester bottles with 300 mL of working volume. 20%, v/v of pre-digested sludge collected from food waste digester was added as an inoculum [40]. The sealed anaerobic digester was incubated at 37 °C, and hydraulic retention time (HRT)—4 days, and organic loading rate (OLR)—1 g VS/L/day was the conditions adopted for the fermentation process. Total solids (TS) and volatile solids (VS) were further quantified, as mentioned by Purser et al. [41] and Esteban-Gutiérrez et al. [42], respectively. The TS content in each reactor was maintained at $13 \pm 0.35\%$, and the VS content in each reactor was maintained at $96 \pm 0.155\%$. VFA was measured as per the standard method [43] by centrifuging the fermented food waste to obtain the sample for VFA estimation [41]. The food waste hydrolysate was then derivatized through methanolysis and given for GC–MS analysis to confirm the presence of butyric and valeric acid [42]. The column used for detection in GC–MS was HP-5MS (5%-phenyl)-methylpolysiloxane, $30 \text{ m} \times 250 \text{ } \mu\text{m} \times 0.25 \text{ } \mu\text{m}$ where the injector temperature was 220 °C Detector temperature: 250 °C; Column temperature: increased from 60 to 150 °C at a rate of 7 °C/min, hold at 150 °C for 5 min, and increased to 230 °C at a rate of 20 °C/min, hold at 230 °C for an additional 10 min.

Fermentation Conditions

The minimal salt media comprised of in (g/L): Na_2HPO_4 -6.8; KH_2PO_4 -3; NaCl -0.5; NH_4Cl -1.05; Citric acid-1.66; $\text{MgSO}_4 \cdot 7\text{H}_2\text{O}$ -1.20; K_2HPO_4 -1.5; NH_4Fe (III) citrate-0.05; yeast extract-0.1; trace element solution-2 mL; in 1 L of cheese whey with an adjusted lactose content of 10 g/L. The trace element solution comprised of (g/L) $\text{FeCl}_3 \cdot 6\text{H}_2\text{O}$ -27; $\text{ZnCl}_2 \cdot 4\text{H}_2\text{O}$ -2; $\text{CoCl}_2 \cdot 6\text{H}_2\text{O}$ -2; $\text{Na}_2\text{MoO}_4 \cdot 2\text{H}_2\text{O}$ -2; $\text{CaCl}_2 \cdot 6\text{H}_2\text{O}$ -1; $\text{CuCl}_2 \cdot 6\text{H}_2\text{O}$ -1.3; H_3BO_3 -0.5; concentrated HCl-100 mL, distilled water-900 mL [44]. Production media comprises various ratios of cheese whey and food waste hydrolysate (v/v ratio) ranging from 100, 90:10, 80:20, 70:30, 60:40, 50:50, and 40:60 (v/v) was prepared to optimize the substrate ratio for maximum biomass and PHBV yield. The pH was adjusted to 7.2, and 10% of the mother inoculum was added to the production media. The fermentation medium was incubated for 72 h in an orbital shaker with a speed of 150 rpm at a constant temperature of 37 °C.

Extraction and Estimation of PHBV

After the 72-h fermentation, the production media was centrifuged at 10,000 rpm for 20 min at 4 °C. The harvested

biomass was further treated with a 6% sodium hypochlorite solution, and an equal amount of chloroform was added, thus maintaining a ratio of 1:1. The solution was vigorously mixed and incubated in an orbital shaker at 37 °C for 1 h. Three different layers were observed. The upper and middle layers (sodium hypochlorite and cell debris) were removed, and the bottom organic layer (chloroform) was evaporated under a fume hood. The extracted PHBV was further quantified gravimetrically [10].

GC–MS Analysis

The PHBV was derivatized through methanolysis to confirm the presence of butyric acid in the extract. Precisely, 20 mg of PHBV was added to 20 ml of 5% (v/v) H_2SO_4 in methanol and transferred to a round bottom flask. This round bottom flask was immersed in a silicone oil bath placed on a heating mantle at 80–90 °C for 6 h. The derivatization setup was arranged, and the reflux was connected to initiate the condensing of vapor. Subsequently, the set up was removed, and the sample was collected. Further, 20 ml of distilled water and chloroform were added to the sample and made to stand in a separating funnel for 20 min. The top layer (organic phase) was procured, filtered using a 0.45 μm syringe filter, and analyzed through GC–MS (Agilent Technologies, GC-7890B, and MS-5977A). The column used for detection in GC–MS was HP-5MS (5%-Phenyl–methyl siloxane, $30 \text{ m} \times 250 \text{ } \mu\text{m} \times 0.25 \text{ } \mu\text{m}$) where the inlet temperature was 170 °C; detector temperature was 200 °C with an increasing rate of 3 °C/min [45, 46].

Batch Kinetics Study of PHBV Production

The optimized media was utilized for performing batch kinetic studies to inspect the parameters that affect the fermentation process beginning right from the 0 h till 120 h. Biomass yield (g/L), PHBV yield (g/L), PHBV content (% g/g) and residual lactose content (g/L) was estimated. Residual lactose content in the medium was estimated by the Anthrone test [45]. Furthermore, kinetic parameters such as $Y_{X/S}$ (g/g), $Y_{P/S}$ (g/g), $Y_{P/X}$ (g/g), ($Y_{P/S}/\text{h}$), and ($Y_{P/X}/\text{h}$) were determined.

Preparation and Characterization of Corncob-Derived Nanocellulose

Alkaline and Acid Treatment of Corncob

The initial untreated corncob residue was ground using a blender to obtain a powder. This powdered corncob was primarily treated with an alkaline solution for purification, where 2% NaOH was added and heated at 70 °C for 1 h. Later, the treated corncob was separated using Whatman

filter paper No. 1, and the residue was kept for drying at 45 °C [47]. The alkaline treated dried corncob samples were mixed with 100 ml of 2% (w/v) sulphuric acid to give a solid to liquid ratio of 1:10. Subsequently, the reaction mixtures were then autoclaved at 130 °C for 20 min. Further, the remaining solid was filtered from the aqueous solution by filtration, and the filtrate (corn cob hydrolysate) was concentrated by vacuum evaporation [32]. The dried corncob samples were then morphologically envisioned using a field emission scanning electron microscope (Quanta 200 FEG FE-SEM) [47].

Nanocellulose Production

The concentrated corncob hydrolysate was then sonicated for 30 min (9 cycles) with power adjusted at 400 Watts required to recover nanocellulose [48]. TEM analysis was performed to confirm the corncob hydrolysates conversion to nanocellulose using a JEM-2100 PLUS (JEOL, Tokyo, Japan) transmission electron microscope with an accelerating voltage of 200 kV equipped with an EDS detector. The sample was prepared by placing a drop of diluted hydrolysate solution on a carbon-coated copper grid followed by drying it at 60 °C before transferring it to the microscope.

Preparation of PHBV Biocomposite

For the preparation of PHBV biocomposite, 50 mg of PHBV was dispersed in 20 mL of chloroform along with nanocellulose hydrolysate; this mixture was subjected to ultrasonication for 30 min to form a homogenous solution, yielding to the formation of PHBV biocomposite. This solution was carefully poured into a petri dish, and the solvent was evaporated at room temperature to obtain a dry powder of PHBV biocomposite [49]. Further, the neat PHBV and the synthesized PHBV biocomposite samples were compared morphologically using a field emission scanning electron microscope (Quanta 200 FEG FE-SEM).

Analytical Methods

FT-IR Analysis

The presence of various functional groups was compared and investigated through FT-IR spectroscopy. The samples with KBr pellets of 10 mm in diameter and 1 mm in thickness were prepared for the analysis. About 5 mg of the prepared PHBV, nanocellulose, and PHBV biocomposite samples were analyzed by Agilent Technologies, Cary 600 Series/ a Perkin-Elmer infrared spectrophotometer between the frequency range of 400–4000 cm^{-1} [50].

XRD Analysis

XRD analysis of PHBV biocomposite (powder) was carried out at room temperature, having a Cu-K α source (Wavelength = 1.54060 Å) and a generator at 40 kV and 15 mA in order to determine the crystalline/amorphous nature of the film and to confirm the presence of nanocellulose in PHBV biocomposite. The samples were analyzed in the scan range of 10°–80° (2 θ) [51]. The crystallinity index (CrI) was calculated by using the diffraction intensities of the crystalline structure and that of the amorphous fraction, according to the method of Segal et al. [52]:

$$\text{CrI\%} = \left[\frac{I_{002} - I_{\text{am}}}{I_{002}} \right] \times 100 \quad (1)$$

where I_{002} is the maximum intensity of the (002) diffraction peak, taken at 2 θ between 22° and 23°, and I_{am} is the intensity of the amorphous diffraction peak taken at 2 θ between 18° and 19°.

Scherrer's equation was used to calculate the crystallite size, T (nm):

$$T = K\lambda/\beta \cdot \cos \theta \quad (2)$$

where K is a dimensionless shape factor and usually taken to be 0.9, λ (1.54 Å) is the X-ray wavelength, β is the line broadening at half the maximum intensity (FWHM), in radians, and θ is the diffraction angle [53].

Analysis of Thermal and Mechanical Characteristics

Firstly, the PHBV biocomposite film was fabricated using the solvent casting method. The dried powder of PHBV biocomposite was dissolved in chloroform to form a homogenous solution and heated at 60–70 °C for 1 h. The solution was then casted on a rectangular glass plate or a glass Petri plate, and the solvent was slowly evaporated at room temperature to obtain the films [44]. The film was subsequently utilized for further characterization. The thermal degradation properties of the biocomposite were analyzed using a thermogravimetric analyzer. The samples were scanned at a temperature gradient of 25 °C to 800 °C at a heating rate of 20 °C min^{-1} . Additionally, the thermal properties like the melting temperature and enthalpy of the synthesized biocomposite were determined using DSC [10]. The samples placed under a nitrogen flow rate of 0.12 L min^{-1} were scanned at a temperature gradient of –30 °C to 300 °C at a heating rate of 10 °C/min. The neat PHBV and PHBV biocomposite films were further used to determine the mechanical properties like tensile strength, Young's modulus, and elongation at break.

Biodegradability Analysis

Biodegradability analysis of PHBV biocomposite and PHBV films were analyzed by soil burial technique [54]. Pre-weighed samples were buried in the soil under a depth of 4–6 cm from the surface. The biodegradability analysis was conducted under an ambient atmospheric condition of 28 °C temperature and 80% relative humidity. Each sample was placed in the soil and withdrawn at an interval of 1 week until the 7th week. After every consecutive week, the samples were retrieved from the soil, washed with distilled water to remove the soil residues on the films, and oven-dried at 60 °C until a constant weight was attained. Prior to and following the degradation, the average percentage of mass loss of each film was calculated from the following equation:

$$\text{Weight reduction (\%)} = \left[(W_i - W_f) / W_i \right] \times 100 \quad (3)$$

where W_i (g) is the initial weight, and W_f (g) is the final weight of the sample [55].

Results and Discussion

Characterization of Food Waste Hydrolysate

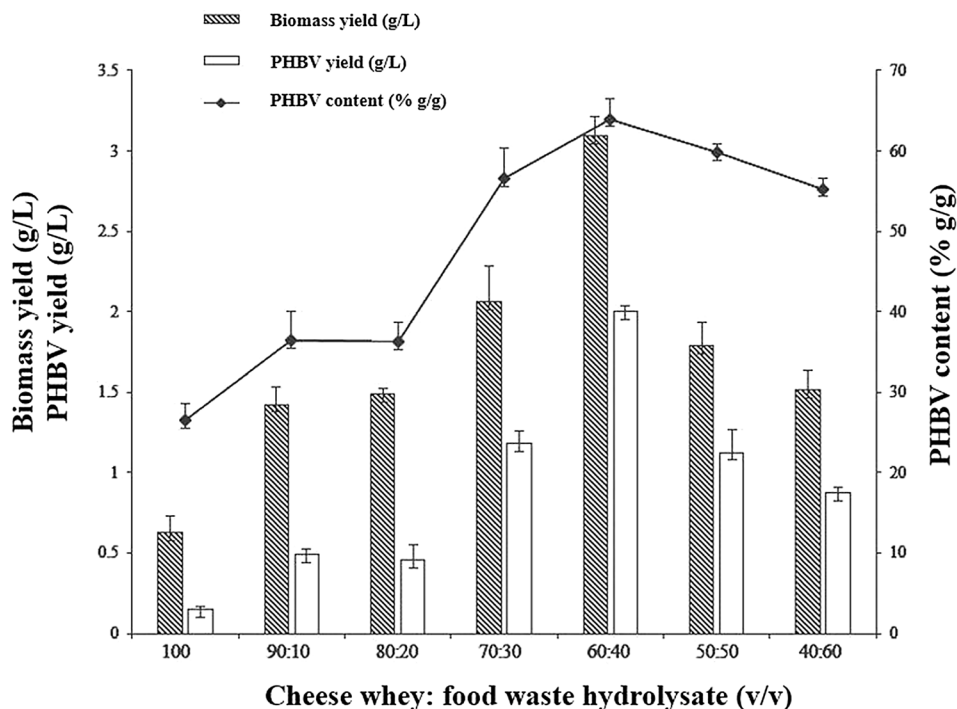
The food waste hydrolysate obtained during AD was analyzed for VFA production. The VFA recovered from the food waste distillate was quantified to be 21 ± 0.48 g/L. The

composition of food waste-derived VFA was determined by GC–MS, and the chromatogram revealed two characteristic peaks. The peak at 4.899 min corresponds to butyric acid methyl ester, and a prominent peak at 7.133 min detected valeric acid methyl ester. These peaks confirmed the presence of butyric acid and valeric acid in the food waste hydrolysate. The food waste hydrolysate obtained during AD contains VFAs, such as propionic acid, butyric acid, and valeric acid [13]. These VFAs present in food waste hydrolysate can act as precursors for the monomeric units like 3HB and 3HV in PHBV copolymer production [9]. Generally, valeric acid or their salt forms are supplemented as precursors for 3HV synthesis [14]. Hence, the presence of valeric acid in the food waste hydrolysate supports the 3HV production and can be a promising supplement in the media when co-fed with cheese whey for the biosynthesis of PHBV by *B. megaterium*.

Optimization of Cheese Whey and Food Waste Hydrolysate Ratio for PHBV Production

The ratio of cheese whey and food waste hydrolysate (v/v) in the production medium was optimized to obtain the maximum biomass and PHBV yield (Fig. 1). From the graph, it is inferred that the biomass yield (g/L) and PHBV yield (g/L) steadily increased until the ratio of 60:40 (v/v) and further decreased drastically. The initial increase in the yield could be due to the uptake of the available carbon in cheese whey and VFA in the food waste hydrolysate to synthesize

Fig. 1 Optimization of cheese whey and food waste hydrolysate ratio (v/v)



the biopolymer, PHBV. The maximum biomass yield and PHBV yield of 3.09 ± 0.12 g/L and 2.0 ± 0.03 g/L respectively correspond to a PHBV content of $64 \pm 2.5\%$ g/g, which were observed at 60:40 (v/v) ratio. The decrease after 60:40 (v/v) ratio probably illustrated the retarded growth of *B. megaterium* due to substrate inhibition, as the biomass yield dropped from 3.09 to 1.5 g/L, and subsequently reducing the PHBV yield to 0.9 g/L until the ratio of 40:60 (v/v). Thus, the optimum ratio of cheese whey and food waste hydrolysate was observed at 60:40 (v/v) ratio. Studies conducted on PHBV production using whole cheese whey as carbon source reported a maximum PHBV yield of 1.2 g/L [56] and utilizing VFA as sole carbon source indicated a yield of 0.57 g/L [13]. Moreover, the study conducted by [57] on supplementing synthetic propionic acid in the medium for PHBV production revealed the PHBV yield ranging from 0.5–2.0 g/L. Hence, combined utilization of cheese whey and food waste hydrolysate (in the ratio of 60:40 v/v) promises an economical and sustainable PHBV production process with higher PHBV yield. The PHBV extracted from *B. megaterium* was characterized by GC–MS, and the chromatogram revealed 3-hydroxybutyric acid methyl ester peak at 4.946 min, and 3-hydroxyvaleric acid methyl ester peak at 6.498 min. This confirmed the presence of both the monomeric units: 3HB and 3HV in the synthesized PHBV. The PHBV copolymer comprises 59% of 3HV monomeric units. The ratio of hydroxyl-butyric acid and hydroxyl-valeric acid monomers significantly impacts qualities such as toughness and flexibility; butyric acid provides stiffness, whereas valeric acid promotes flexibility to PHBV. The high percent of the 3HV monomeric unit in PHBV brings comparatively higher flexibility than PHB and can have a potential advantage in applications like packaging industries.

Batch Kinetics Study of PHBV Production

Batch kinetic studies were conducted for 120 h to observe the relation between cellular growths, PHBV production, PHBV accumulation, and lactose utilization from cheese whey. The batch kinetic graph (Fig. 2a) revealed the trend of biomass yield, PHBV yield, PHBV content, and residual lactose content for varying time (0–120 h). The biomass yield increased from 1.25 ± 0.3 g/L to 2.05 ± 0.2 g/L during the exponential growth phase. The highest biomass yield of 3.05 ± 0.07 g/L was obtained at 72 h, after which the growth declined until 120 h. A similar pattern was observed in PHBV yield, which reported a maximum yield of 2.175 ± 0.06 g/L at 72 h. The PHBV content increased exponentially from the 48 h and reached a maximum of 71.43% at 72 h. The decline in the PHBV yield and PHBV content after 72 h is a direct consequence of reducing the intracellular accumulation of PHBV due to retarded growth

of *B. megaterium* after 72 h. Thus, the maximum production of biomass and PHBV was reported at the time of 72 h. Moreover, the rapid utilization of lactose decreased from an initial value of 10.11 ± 0.12 g/L to 0.61 ± 0.001 g/L, which indicated the active uptake of lactose by *B. megaterium*. The residual lactose concentration (g/L) in the medium was steady after 72 h, indicating the saturation in the utilization of lactose for growth and PHBV production.

The growth rate (μ) of *B. megaterium* was found to be equal to 0.02 h⁻¹. The kinetic parameters involved in the synthesis of PHBV, such as yield coefficients ($Y_{X/S}$, $Y_{P/X}$, and $Y_{P/S}$) and productivity ($Y_{P/S}$ /h, and $Y_{P/X}$ /h), were estimated from the batch kinetic study. The graph (Fig. 2b) showed a similar trend for the yield coefficients of biomass and product with respect to the substrate ($Y_{X/S}$, $Y_{P/S}$). $Y_{X/S}$ and $Y_{P/S}$ increased from 24 to 72 h with the maximum value of 0.428 g/g and 0.30 g/g respectively at 72 h and further decreased until 120 h. This was due to the increase in the synthesis of PHBV in the stationary phase by *B. megaterium*. The product's yield coefficient concerning biomass ($Y_{P/X}$) steadily increases from 24 to 120 h with a maximum value of 0.7890 g/g. The PHBV productivity related to substrate and biomass ($Y_{P/S}$ /h and $Y_{P/X}$ /h) presented a similar trend. The productivities increased steadily until 48 h with a maximum value of 0.0063 h⁻¹ and 0.0148 h⁻¹, followed by a rapid decrease until the 120 h. This indicates the rapid utilization of the substrate and a cumulative increase in the organism's growth for the synthesis of PHBV. Thus, the exponential growth phase of *B. megaterium* was achieved until 48 h, as the biomass increased steadily by utilizing the substrate for its growth. The biopolymer PHBV was synthesized during the stationary phase between 48 and 72 h, where the product yield was obtained maximum at 72 h (2.175 ± 0.06 g/L), which validated that PHBV is a secondary metabolite. Similar observations were corroborated in studies conducted by [58], which reported 2.2 g/L of PHBV produced by *B. megaterium* from whole whey medium enriched with glucose. Studies conducted on the production of PHBV utilizing VFA as sole carbon source has reported biomass production of 1.5 ± 0.06 g/L, and a $27.4 \pm 2\%$ PHAs accumulation [13]. Additionally, Bhatia et al. [13] revealed lower $Y_{X/S}$, $Y_{P/S}$ yields of 0.10 ± 0.003 g/g, and 0.11 ± 0.002 g/g, respectively. The current study discloses a higher PHBV and biomass production by co-utilizing cheese whey and food waste-derived VFA, paving the way for modeling a sustainable PHBV production process.

Nanocellulose Derived from Corncob

SEM Analysis of Untreated and Treated Corncob

Scanning electron microscopy (SEM) examined the surface morphology of corncob before and after acid treatment

Fig. 2 **a** Batch kinetics study of PHBV production, **b** Analysis of kinetic parameters

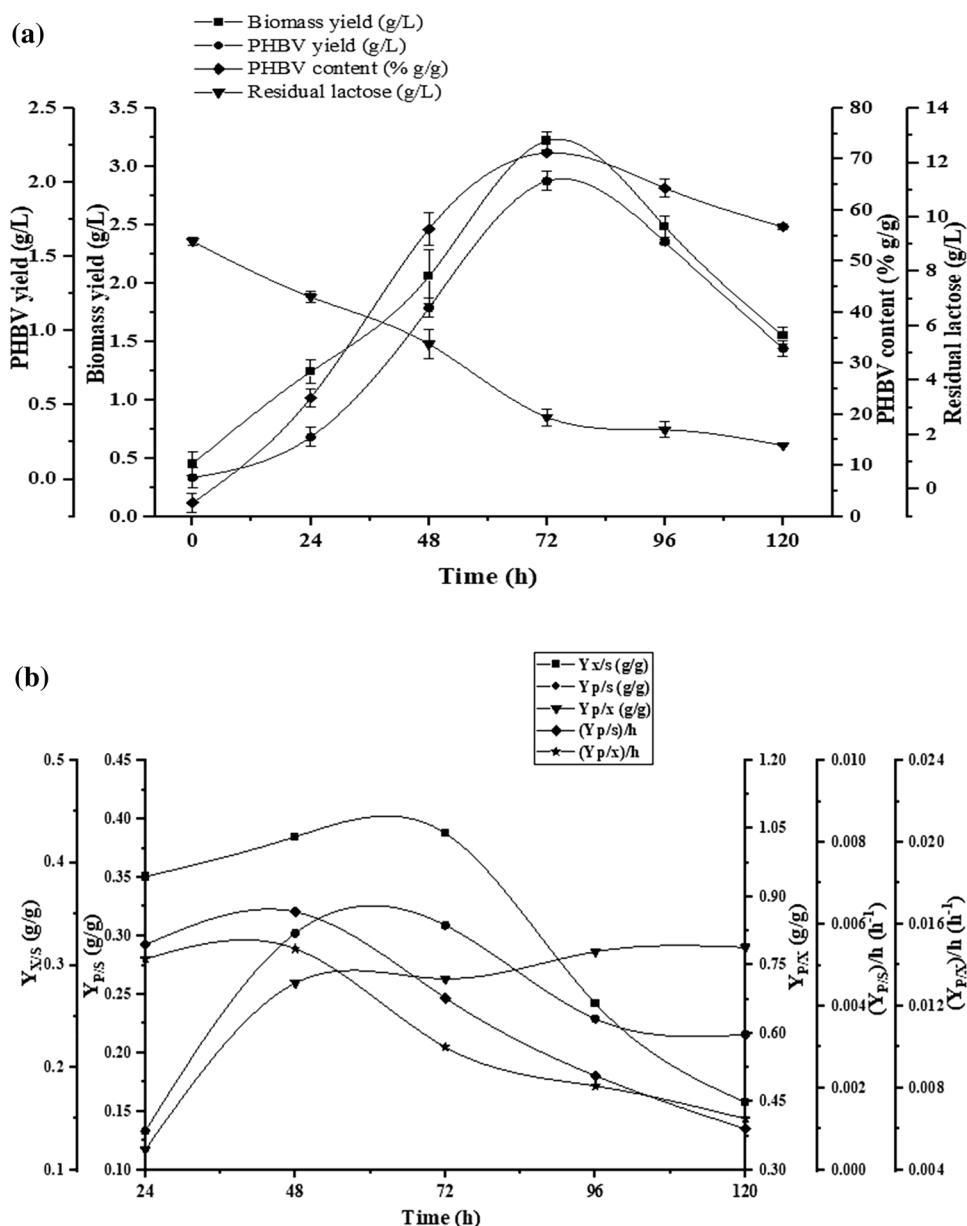


(Fig. 3a, b). The smooth and compact structure could be observed in the untreated corncob (Fig. 3a). However, the corncob treated with sulphuric acid had relatively rough surfaces throughout it (Fig. 3b). The rough surface in Fig. 3b exhibited the removal of the structural components. This observation suggests that the acidified treatment was beneficial for separating cellulose from the corncob [47, 59]. Additionally, it indicates that the acid treatment was effective for removing cellulose from corncob [60]. Moreover, the acid hydrolysate derived from corncob was estimated with 63 wt% of cellulose, which reveals the extraction of cellulose from the corncob. This result substantiates the effectiveness of the treatment with sulphuric acid to obtain cellulose.

TEM Analysis of Corncob-Derived Nanocellulose

The nanocellulose obtained from the acid hydrolysate of corncob after mechanical dispersion was analyzed for the size reduction under transmission electron microscopy (TEM). The TEM image verified the presence of globular-shaped nanometric particles at a range of 50 nm (Fig. 4a). A prominent peak with a maximum percentage of carbon in the EDS (Energy-dispersive X-ray spectroscopy) spectrum was observed, which reveals the presence of cellulose in the nano form (Fig. 4b). The TEM images of nanocellulose were similar to those derived from sulphuric acid hydrolysis of various sources such as paper pulp, rice straws, and wheat straws [61, 62]. A study conducted by do Lago et al. [60] reported

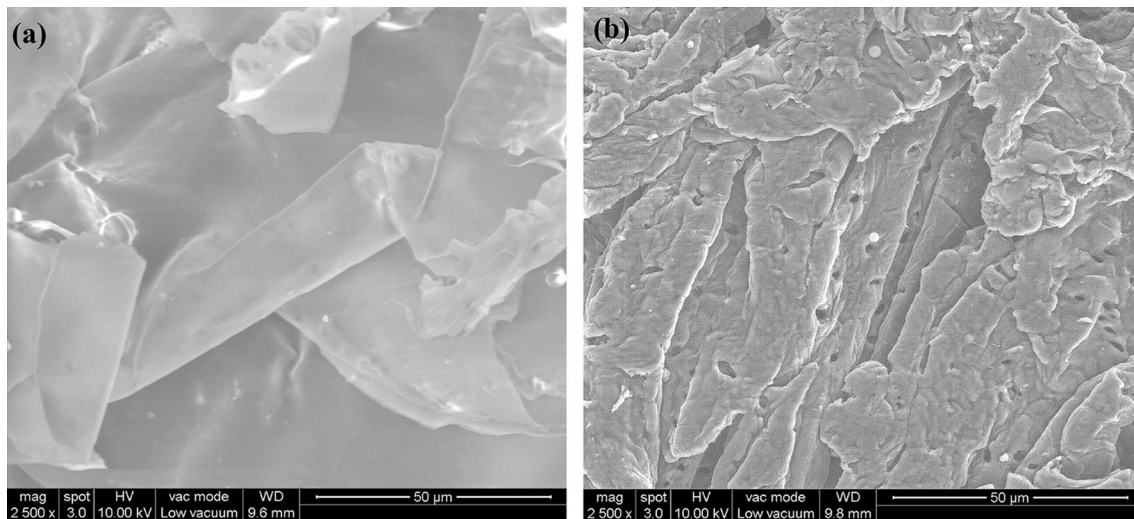


Fig. 3 SEM images of **a** untreated corncob, **b** acid-treated corncob

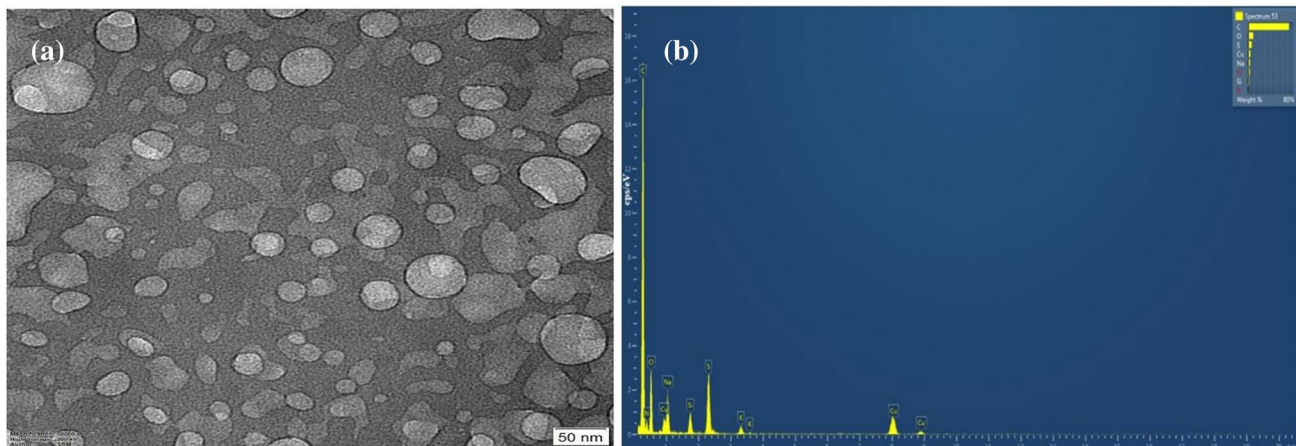


Fig. 4 **a** TEM image of nanocellulose, **b** EDS analysis of nanocellulose

that the biocomposites comprise a matrix of biopolymer reinforced with nanoparticles between the nanoscale ranges of 1–100 nm. TEM images reveal the nano-scaling of the cellulose to the range of approximately 50 nm, thus ensuring its application as a reinforcing agent for the biosynthesized PHBV. According to Zhou et al. [63], nanocellulose with this diameter range is suitable for strengthening biopolymers. Moreover, the TEM analysis ensures the conversion of a higher percentage of cellulose in the nanoscale (nanocellulose) by mechanical dispersion of the acid hydrolysate and integrating this corncob-derived nanocellulose in PHBV to produce PHBV biocomposite.

Physical and Chemical Characterization

SEM Analysis of PHBV and PHBV Biocomposite

SEM analysis of neat PHBV (Fig. 5a) and PHBV biocomposite (Fig. 5b) illustrates their morphological difference. The surfaces of neat PHBV exhibited comparatively more fractures on the matrix than the PHBV biocomposite, revealing that the addition of nanocellulose enhanced the crosslinking in the PHBV biocomposite, which was absent in the neat PHBV due to the lack of reinforcement (with nanocellulose) [64]. The PHBV biocomposites (reinforced with nanocellulose) displayed nanocellulose adhering firmly to the PHBV matrix with no pores or fractures, ensuring strong interfacial adhesion between the PHBV matrix and

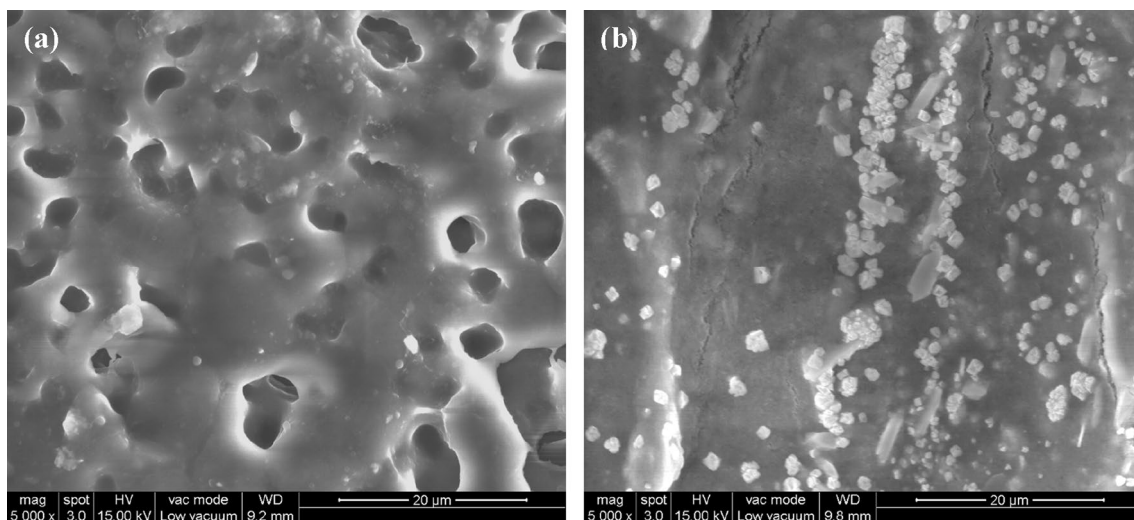


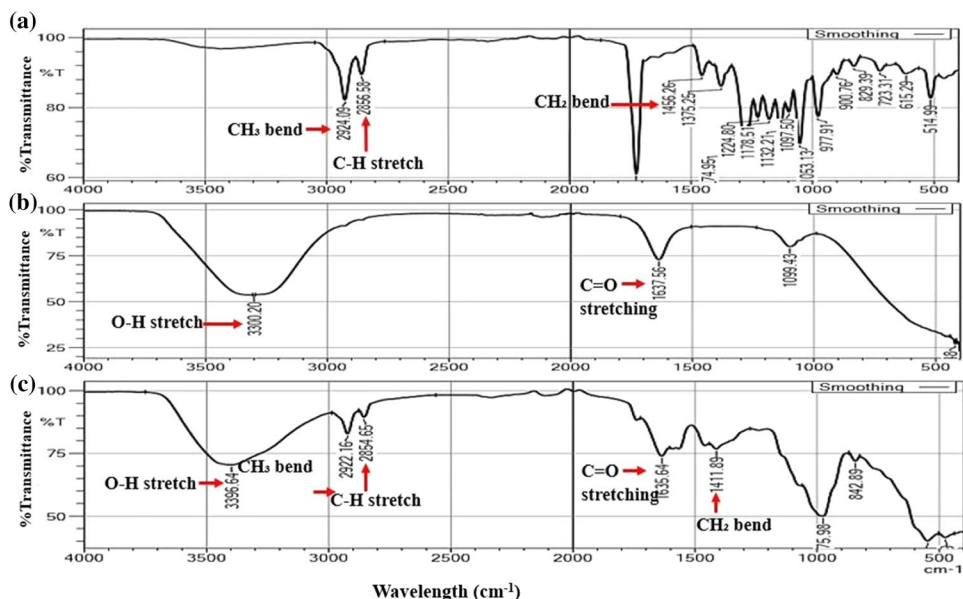
Fig. 5 SEM images of **a** PHBV, **b** PHBV biocomposite

nanocellulose in the PHBV biocomposite [65]. Moreover, some roughness on the surface of the biocomposite film (Fig. 5b) was visualized, probably due to the agglomeration of nanocellulose, which were randomly dispersed on the PHBV matrix to compose the film. The biocomposite film had formed a continuous network of hydrogen bonds between the nanocellulose and PHBV along the film's entire surface; thus, no fractures or punctures were observed. Thus, the improved interfacial adhesion of nanocellulose on PHBV biocomposite was strong enough to transfer the stresses from the PHBV matrix to the nanocellulose, which was supported and evidenced by the mechanical characterization of the films as discussed in the later section.

FT-IR Analysis

FT-IR spectra of PHBV, nanocellulose, and PHBV biocomposite were obtained and compared with each other to determine the functional groups involved (Fig. 6a–c). The functional groups present in PHBV, nanocellulose, and PHBV biocomposite are revealed from the FT-IR spectra. A prominent broad peak of nanocellulose and PHBV biocomposite at 3300.20 cm^{-1} and 3396.64 cm^{-1} assigned to hydroxyl groups (O–H stretch). The spectra of PHBV and PHBV biocomposite at 2856.88 cm^{-1} and 2854.65 cm^{-1} represents the C–H stretching of alkanes. The peak at 1637.56 cm^{-1} and 1635.64 cm^{-1} is attributed to the amide group's C=O

Fig. 6 FT-IR analysis of **a** PHBV, **b** nanocellulose, **c** PHBV biocomposite



stretching in nanocellulose and PHBV biocomposite. Additionally, both PHBV and PHBV biocomposite spectra show a peak of C–H stretching of a methyl group at 2924.09 cm^{-1} and 2922.16 cm^{-1} , respectively, and the peaks 1456.26 cm^{-1} and 1411.89 cm^{-1} indicates the C–H bending methylene groups, respectively [44]. These characteristic peaks (C–H stretching, C=O stretching) of PHBV biocomposite closely resembles the peaks of PHBV, confirming their similarity based on the chemical composition. The shifting peaks observed in the biocomposite indicates the occurrence of the chemical reaction between the nanocellulose and PHBV [66]. These observations suggested that successful reinforcement between the matrix (PHBV) and nanocellulose was achieved [67].

XRD Analysis

The crystalline nature of PHBV and PHBV biocomposite was studied by XRD analysis. Figure 7 shows diffraction patterns of both PHBV and PHBV biocomposite. The diffractogram of PHBV biocomposite revealed two significant peaks of at diffraction angle $2\theta = 13.4^\circ$ and 16.9° , and the diffractogram of PHBV displayed similar peaks at diffraction angle $2\theta = 13.4^\circ$ and 17.0° , showing the typical crystalline structure of PHBV in both the films. The characteristic peaks were observed in the biocomposite at diffraction angle $2\theta = 22.8^\circ$, 25.6° , and 26.0° , which represents the cellulosic crystalline peak [51, 68]. The crystalline nature of PHBV and its biocomposite materials significantly affect their mechanical properties as well as processability [69]. The crystallinity index (CrI) of both PHBV and PHBV biocomposite was evaluated as 21.8% and 36.6%, respectively. This increase in CrI of PHBV biocomposite depicted the increment in the crystallinity of the polymer biocomposite, resulting in the exposure of crystalline nanocellulose in PHBV biocomposite [47]. It is worth noting that the crosslinking of the nanocellulose and the PHBV matrix

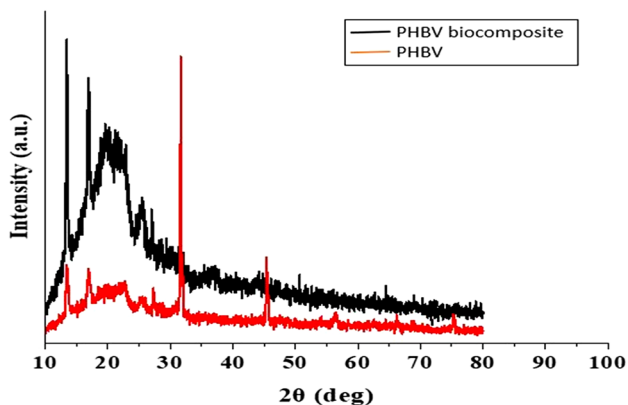


Fig. 7 XRD analysis of PHBV and PHBV biocomposite

attributed to the increase in biocomposites' crystallinity, which would improve the compatibility between cellulose and the biopolymer. Moreover, the crystallite size (T) of PHBV and PHBV biocomposite was determined as 66.1 nm and 27.9 nm, respectively. The reduction in the crystallite size was observed due to the incorporation of nanocellulose in PHBV biocomposite, as nanoparticles exhibit smaller crystallite size [53]. Hence, the PHBV biocomposite manifested superior crystalline properties than PHBV, due to the incorporation of nanocellulose. Similar XRD patterns were observed in biocomposites/nanocomposites, including PHBV/ α -Cellulose blend [70] and PLA/PHBV nanocomposite [17]. The XRD peaks in the present study confirmed the presence of nanocellulose and PHBV in the biocomposite.

Thermal Characterization of PHBV Biocomposite

Thermogravimetric Analysis (TGA)

The thermal degradation of the PHBV biocomposite film sample is shown in Fig. 8a. The thermogram depicted an initial degradation at 181.46°C , with the moisture weight loss of 3.36 wt%. This was followed by a sudden weight loss of about 95.88% up to 595.32°C due to the biopolymer decomposition. The thermo-labile components were completely degraded at this temperature. The peak degradation temperature was found at 790°C , corresponding to the highest decomposition with a 4.1 wt% residual mass. From the previous study by Suhazsini et al. [10], the PHBV showed a peak degradation temperature of 508.82°C , with a residual mass of approximately 51%. The presence of hydroxyl groups on the surface of cellulose acted as sites of nucleation for PHBV, which was considered as the foremost cause of the biocomposite's rapid degradation. The current study reveals that the PHBV biocomposite can withstand high degradation temperature with the maximum decomposition of the sample compared to the biosynthesized P(3HB) by *B. megaterium* [58], and PHB/Cellulose fibers composites [71]. Yu et al. [72] conducted similar studies on PHBV/Cellulose nanocrystals nanocomposites and reported comparatively less T_{max} of 292.9°C . As stated by the authors, the improvement in the thermal stability was due to the intermolecular hydrogen bonding interactions between the nanocellulose and PHBV. Thus, the thermal stability of PHBV biocomposite has been enhanced due to the reinforcement of the nanocellulose.

Differential Scanning Calorimetry (DSC)

The DSC thermogram reveals the nature of the biocomposite during phase transition when external heat is applied. The heat flow was analyzed in accordance with the temperature where the peak temperature or the melting temperature (T_m)

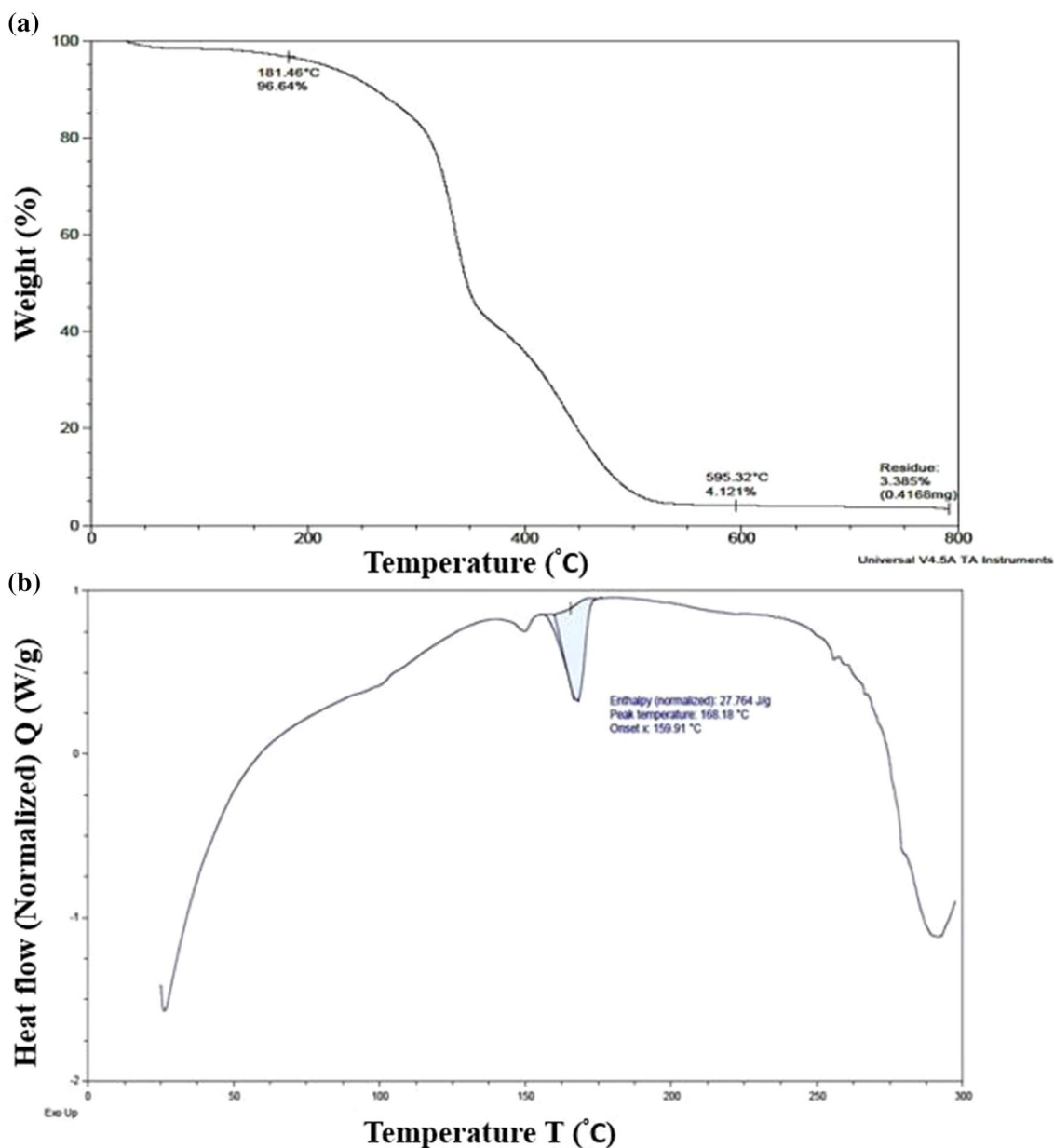
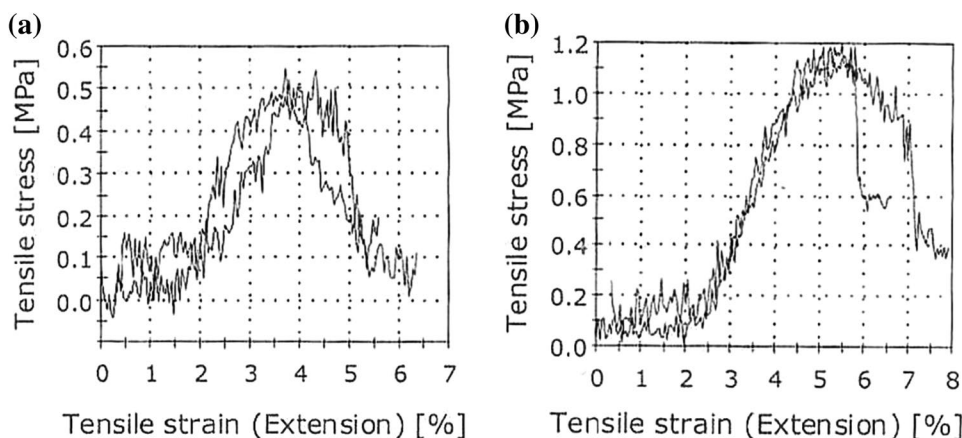


Fig. 8 a TGA of PHBV biocomposite, b DSC of PHBV biocomposite

was observed to be 168.18 °C (Fig. 8b). The PHBV biocomposite showed higher enthalpy of 27.7 J/g compared to neat PHBV (19.3 J/g), emphasizes the role of nanocellulose in improving the crystallization and acts as a crystallization nucleus. In comparing the neat PHBV with PHBV biocomposite, it was observed that the enthalpy was increased drastically with the incorporation of nanocellulose, which indicated that the nanocellulose facilitates the crystallization process [71]. The dispersion of nanocellulose in the PHBV matrix acts as nuclei sites to form a critical nucleus [69].

This property is essential for the improved mechanical performance of the biocomposite. The melting temperature (T_m) of the PHBV biocomposite was relatively higher than that of the PHBV, which was 116.6 °C, as reported by Suhazsini et al. [10]. This would have been caused due to the nanocellulose reinforcement in the biocomposite and interactions between the nanocellulose and PHBV matrix.

Fig. 9 Stress–strain curve of **a** PHBV, **b** PHBV biocomposite**Table 1** Mechanical properties of PHBV and PHBV biocomposite

Sample	Tensile strength (MPa)	Elongation at break (%)	Young's Modulus (MPa)
PHBV	7.10	3.85	15
PHBV biocomposite	11.11	5.31	40

Mechanical Characterization of PHBV Biocomposite

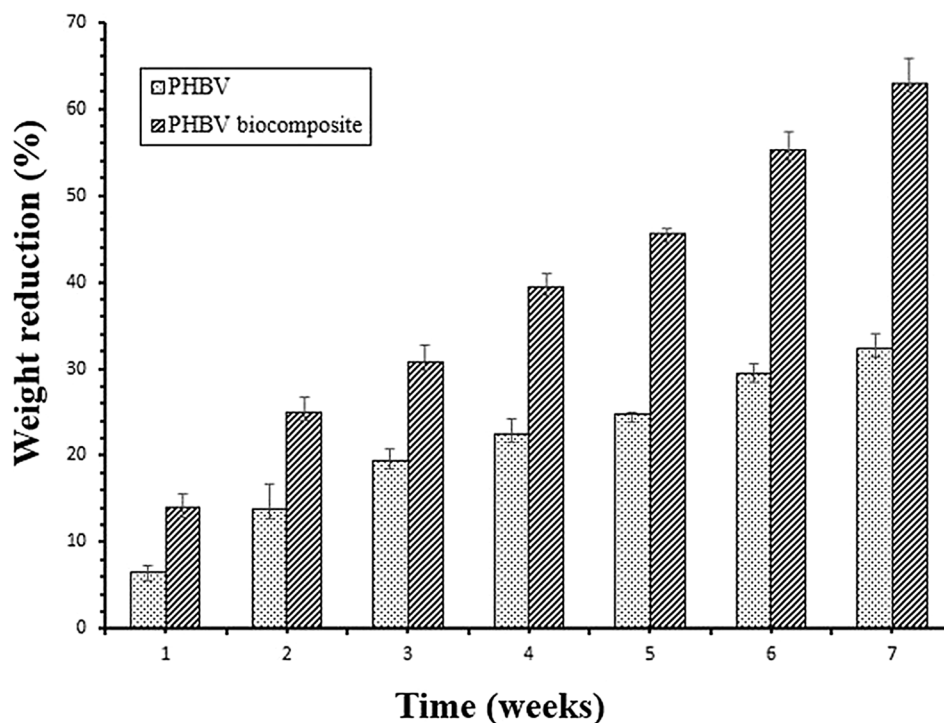
The mechanical properties were compared between PHBV and PHBV biocomposite, and various mechanical parameters such as tensile strength (σ_y), Young's modulus (E), and elongation at break (ϵ_b) was calculated based on the stress–strain curve (Fig. 9a, b). The tensile strength of the biocomposite film was 11.11 MPa, which was comparatively higher than that of standard PHBV (7.10 MPa). The results obtained for tensile strength of the biocomposite were similar or superior to those presented by Low-Density Polyethylene (Tensile strength = 6.9–16 MPa) [60], polymers traditionally used in the food industry and agricultural sector. PHBV biocomposite exhibited higher Young's modulus of 40 MPa and 5.3% elongation at break, which is higher than the PHBV (Table 1). These properties attribute to its higher flexibility and deformation rate. Thus, the improvement in these properties of biocomposites is substantiated with the addition of corn-cob-derived nanocellulose. These parameters represented clear evidence of the good dispersibility of nanocellulose in the PHBV polymeric matrix, as reported by Makaremi et al. [73] and Mazur et al. [35]. Compared to the biosynthesized PHBV by *B. megaterium*, the PHBV biocomposite shows improved mechanical properties [36]. The enhanced mechanical properties of PHBV biocomposite

proves that the nanocellulose can be employed as a reinforcing agent.

Biodegradability Analysis

Both PHBV and PHBV biocomposite samples gradually decomposed, and the weight reduction (%) pattern was observed with respect to time of degradation (weeks) (Fig. 10). The weight reduction trend of PHBV biocomposite increased rapidly, whereas the neat PHBV depicted a steady weight loss pattern. Within 4 weeks, the PHBV biocomposite displayed faster degradation as the weight reduction percentage increased approximately up to 40%, whereas the neat PHBV merely reached 22%. By the 5th week of degradation, the PHBV biocomposite had developed pores and fragmented, while the PHBV was less fragmented, indicating its comparatively slower degradation. By this time, the weight reduction of PHBV biocomposite reached up to 45.6%, whereas PHBV was reduced by 24.8%. However, in the 7th week of degradation, the weight reduction percentage of PHBV biocomposite reached up to 63%, whereas no considerable change was visualized in the PHBV sample. The neat PHBV revealed a weight loss of 32.4%, which was comparatively less than the PHBV biocomposite. It is worth noting that the weight reduction pattern of PHBV and PHBV biocomposite signified the higher biodegradation rate of PHBV biocomposite than the PHBV, which inferred that the incorporation of nanocellulose significantly affected the degradation rate [4, 65]. The biodegradation percentage of biocomposite was observed to be higher than the previously reported studies of PHBV based composites [1] and commercial polymer like polycaprolactone [55], considering the same time duration. The incorporation of the corn-cob-derived nanocellulose could influence the increased biodegradability of PHBV biocomposite.

Fig. 10 Weight reduction pattern of PHBV and PHBV biocomposite



Conclusion

The biosynthesis of PHBV by *B. megaterium* was carried out by the co-utilization of cheese whey and food waste hydrolysate, which demonstrated a sustainable production process. The high lactose content in cheese whey was utilized by *B. megaterium* to metabolize 3HB units. In contrast, the food waste hydrolysate containing VFAs such as butyric acid and valeric acid was the primary source for producing 3HV units in PHBV. The substrates' optimum ratio was achieved at 60:40 (v/v), with a maximum PHBV yield of 2.0 ± 0.3 g/L and PHBV content of $69 \pm 2.5\%$ g/g. The PHBV biocomposite was obtained by integrating corn-cob-derived nanocellulose into the synthesized PHBV. The tensile strength of PHBV biocomposite (11.11 MPa) was significantly higher than the PHBV (7.10 MPa). Moreover, the PHBV biocomposite revealed higher thermal stability and can withstand high degradation temperature (790 °C), with the maximum decomposition of 95.9%. These enhanced mechanical and thermal properties of PHBV biocomposite prove its biocompatibility and biostability and validates the employment of corn-cob-derived nanocellulose as a reinforcing agent. Moreover, the PHBV biocomposite manifests as a biodegradable polymer with a higher biodegradation rate than various biopolymers. The present study's outcome paves the way for large-scale production of the biocomposite and in exploring its feasibility in various sectors to eradicate the need for plastic-based materials.

Acknowledgements The authors wish to express their sincere thanks to the Department of Biotechnology, SRM Institute of Science and Technology for providing research and analytical facilities. We acknowledge the HRTEM and XRD facility at SRMIST set up with support from MNRE (Project No.31/03/2014-15/PVSE-R&D), Government of India.

Compliance with Ethical Standards

Conflict of interest The authors declare that they have no conflict of interest.

References

- David G, Michel J, Gastaldi E, Gontard N, Angellier-Coussy H (2020) How vine shoots as fillers impact the biodegradation of PHBV-based composites. *Int J Mol Sci* 21(1):228. <https://doi.org/10.3390/ijms21010228>
- Israni N, Shivakumar S (2019) Polyhydroxyalkanoates in packaging. In: *Biotechnological applications of polyhydroxyalkanoates*. Singapore, pp 363–388. https://doi.org/10.1007/978-981-13-3759-8_14
- Bugnicourt E, Cinelli P, Lazzeri A, Alvarez VA (2014) Polyhydroxyalkanoate (PHA): review of synthesis, characteristics, processing and potential applications in packaging. *Express Polym Lett* 8(11):791–808. <https://doi.org/10.3144/expresspolymlett.2014.82>
- Lammi S, Gastaldi E, Gaubiac F, Angellier-Coussy H (2019) How olive pomace can be valorized as fillers to tune the biodegradation of PHBV based composites. *Polym Degrad Stabil* 166:325–333. <https://doi.org/10.1016/j.polymdegradstab.2019.06.010>
- Yang H, Li J, Du G, Liu L (2017) Microbial production and molecular engineering of industrial enzymes: challenges and strategies. In: *Biotechnology of microbial enzymes*. Academic Press, pp. 151–165. <https://doi.org/10.1016/B978-0-12-803725-6.00006-6>

6. Phasakanon J, Chookietwattana K, Dararat S (2014) Polyhydroxyalkanoate production from sequencing batch reactor system treating domestic wastewater mixed with glycerol waste. *APCBEE Proc* 8:161–166. <https://doi.org/10.1016/j.apcbee.2014.03.020>
7. Zhu C, Nomura CT, Perrotta JA, Stipanovic AJ, Nakas JP (2010) Production and characterization of poly-3-hydroxybutyrate from biodiesel-glycerol by *Burkholderia cepacia* ATCC 17759. *Bio-technol Progr* 26(2):424–430. <https://doi.org/10.1002/btpr.355>
8. Koller M, Salerno A, Muhr A, Reiterer A, Chiellini E, Casella S, Horvat P, Braunegg G (2012) Whey lactose as a raw material for microbial production of biodegradable polyesters. In: *Polyester*. InTech, London, pp 51–92. <https://doi.org/10.5772/48737>
9. Kumar G, Ponnusamy VK, Bhosale RR, Shobana S, Yoon JJ, Bhatia SK, Banu JR, Kim SH (2019) A review on the conversion of volatile fatty acids to polyhydroxyalkonates using dark fermentative effluents from hydrogen production. *Bioresource Technol*. <https://doi.org/10.1016/j.biortech.2019.121427>
10. Suhazsini P, Keshav R, Narayanan S, Chaudhuri A, Radha P (2020) A study on the synthesis of poly (3-hydroxybutyrate-co-3-hydroxyvalerate) by *Bacillus megaterium* utilizing cheese whey permeate. *J Polym Environ* 2:1–6. <https://doi.org/10.1007/s10924-020-01687-x>
11. Wang P, Chen XT, Qiu YQ, Liang XF, Cheng MM, Wang YJ, Ren LH (2019) Production of polyhydroxyalkanoates by halotolerant bacteria with volatile fatty acids from food waste as carbon source. *Biotechnol Appl Bioc*. <https://doi.org/10.1002/bab.1848>
12. Shen L, Hu H, Ji H, Cai J, He N, Li Q, Wang Y (2014) Production of poly (hydroxybutyrate–hydroxyvalerate) from waste organics by the two-stage process: focus on the intermediate volatile fatty acids. *Bioresource Technol* 166:194–200. <https://doi.org/10.1016/j.biortech.2014.05.038>
13. Bhatia SK, Gurav R, Choi TR, Jung HR, Yang SY, Song HS, Jeon JM, Kim JS, Lee YK, Yang YH (2019) Poly (3-hydroxybutyrate-co-3-hydroxyhexanoate) production from engineered *Ralstonia eutropha* using synthetic and anaerobically digested food waste derived volatile fatty acids. *Int J Biol Macromol* 133:1. <https://doi.org/10.1016/j.ijbiomac.2019.04.083>
14. Bhubalan K, Rathi DN, Abe H, Iwata T, Sudesh K (2010) Improved synthesis of P (3HB-co-3HV-co-3HHx) terpolymers by mutant *Cupriavidus necator* using the PHA synthase gene of *Chromobacterium* sp. USM2 with high affinity towards 3HV. *Polym Degrad Stabil* 95(8):1436–1442. <https://doi.org/10.1016/j.polymdegradstab.2009.12.018>
15. Abitbol T, Rivkin A, Cao Y, Nevo Y, Abraham E, Ben-Shalom T, Lapidot S, Shoseyov O (2016) Nanocellulose, a tiny fiber with huge applications. *Curr Opin Biotech* 39:76–88. <https://doi.org/10.1016/j.copbio.2016.01.002>
16. Ravindran L, Sreekala MS, Thomas S (2019) Novel processing parameters for the extraction of cellulose nanofibres (CNF) from environmentally benign pineapple leaf fibres (PALF): structure-property relationships. *Int J Biol Macromol* 131:858–870. <https://doi.org/10.1016/j.ijbiomac.2019.03.134>
17. Dasan YK, Bhat AH, Ahmad F (2017) Polymer blend of PLA/PHBV based bionanocomposites reinforced with nanocrystalline cellulose for potential application as packaging material. *Carbohydr Polym* 157:1323–1332. <https://doi.org/10.1016/j.carbpol.2016.11.012>
18. Sarasini F, Luzi F, Dominici F, Maffei G, Iannone A, Zuorro A, Lavecchia R, Torre L, Carbonell-Verdu A, Balart R, Puglia D (2018) Effect of different compatibilizers on sustainable composites based on a PHBV/PBAT matrix filled with coffee silverskin. *Polymers* 10(11):1256. <https://doi.org/10.3390/polym10111256>
19. Quiles-Carrillo L, Montanes N, Sammon C, Balart R, Torres-Giner S (2018) Compatibilization of highly sustainable polylactide/almond shell flour composites by reactive extrusion with maleinized linseed oil. *Ind Crop Prod* 111:878–888. <https://doi.org/10.1016/j.indcrop.2017.10.062>
20. Guna V, Ilangovan M, Hu C, Venkatesh K, Reddy N (2019) Valorization of sugarcane bagasse by developing completely biodegradable composites for industrial applications. *Ind Crop Prod* 131:25–31. <https://doi.org/10.1016/j.indcrop.2019.01.011>
21. Muthuraj R, Lacoste C, Lacroix P, Bergeret A (2019) Sustainable thermal insulation biocomposites from rice husk, wheat husk, wood fibers and textile waste fibers: Elaboration and performances evaluation. *Ind Crop Prod* 135:238–245. <https://doi.org/10.1016/j.indcrop.2019.04.053>
22. Guna V, Ilangovan M, Rather MH, Giridharan BV, Prajwal B, Krishna KV, Venkatesh K, Reddy N (2020) Groundnut shell/rice husk agro-waste reinforced polypropylene hybrid biocomposites. *J Build Eng* 27:100991. <https://doi.org/10.1016/j.job.2019.100991>
23. Ferri M, Vannini M, Ehrnell M, Eliasson L, Xanthakis E, Monari S, Sisti L, Marchese P, Celli A, Tassoni A (2020) From winery waste to bioactive compounds and new polymeric biocomposites: a contribution to the circular economy concept. *J Adv Res*. <https://doi.org/10.1016/j.jare.2020.02.015>
24. Li M, Cheng YL, Fu N, Li D, Adhikari B, Chen XD (2014) Isolation and characterization of corn cob cellulose fibers using microwave-assisted chemical treatments. *Int J Food Eng* 10(3):427–436. <https://doi.org/10.1515/ijfe-2014-0052>
25. Panchal P, Ogunsona E, Mekonnen T (2019) Trends in advanced functional material applications of nanocellulose. *Processes* 7(1):10. <https://doi.org/10.3390/pr7010010>
26. Xue Y, Mou Z, Xiao H (2017) Nanocellulose as a sustainable biomass material: structure, properties, present status and future prospects in biomedical applications. *Nanoscale* 9(39):14758–14781. <https://doi.org/10.1039/C7NR04994C>
27. Kallel F, Bettaieb F, Khiari R, García A, Bras J, Chaabouni SE (2016) Isolation and structural characterization of cellulose nanocrystals extracted from garlic straw residues. *Ind Crop Prod* 87:287–296. <https://doi.org/10.1016/j.indcrop.2016.04.060>
28. Novo LP, Bras J, García A, Belgacem N, Curvelo AA (2015) Subcritical water: a method for green production of cellulose nanocrystals. *ACS Sustain Chem Eng* 3(11):2839–2846. <https://doi.org/10.1021/acssuschemeng.5b00762>
29. Salas C, Nypelö T, Rodriguez-Abreu C, Carrillo C, Rojas OJ (2014) Nanocellulose properties and applications in colloids and interfaces. *Curr Opin Colloid Int* 19(5):383–396. <https://doi.org/10.1016/j.cocis.2014.10.003>
30. Habibi Y, Lucia LA, Rojas OJ (2010) Cellulose nanocrystals: chemistry, self-assembly, and applications. *Chem Rev* 110(6):3479–3500. <https://doi.org/10.1021/cr900339w>
31. Brinchi L, Cotana F, Fortunati E, Kenny JM (2013) Production of nanocrystalline cellulose from lignocellulosic biomass: technology and applications. *Carbohydr Polym* 94(1):154–169. <https://doi.org/10.1016/j.carbpol.2013.01.033>
32. Jeevan P, Nelson R, Rena AE (2011) Optimization studies on acid hydrolysis of corn cob hemicellulosic hydrolysate for microbial production of xylitol. *J Microbiol Biotechnol* 1(4):114–123
33. Wulandari WT, Rochliadi A, Arcana IM (2016). Nanocellulose prepared by acid hydrolysis of isolated cellulose from sugarcane bagasse. In: *IOP conference series: materials science and engineering 2016*, vol 107(1), p 012045. IOP Publishing. <https://doi.org/10.1088/1757-899X/107/1/012045>
34. Kaushik A, Singh M, Verma G (2010) Green nanocomposites based on thermoplastic starch and steam exploded cellulose nanofibrils from wheat straw. *Carbohydr Polym* 82(2):337–345. <https://doi.org/10.1016/j.carbpol.2010.04.063>
35. Mazur K, Kuciel S (2019) Mechanical and hydrothermal aging behaviour of polyhydroxybutyrate-co-valerate (PHBV)

- composites reinforced by natural fibres. *Molecules* 24(19):3538. <https://doi.org/10.3390/molecules24193538>
36. Martínez-Sanz M, Villano M, Oliveira C, Albuquerque MG, Majone M, Reis M, Lopez-Rubio A, Lagaron JM (2014) Characterization of polyhydroxyalkanoates synthesized from microbial mixed cultures and of their nanobiocomposites with bacterial cellulose nanowhiskers. *New Biotechnol* 31(4):364–376. <https://doi.org/10.1016/j.nbt.2013.06.003>
 37. Seoane IT, Fortunati E, Puglia D, Cyras VP, Manfredi LB (2016) Development and characterization of bionanocomposites based on poly (3-hydroxybutyrate) and cellulose nanocrystals for packaging applications. *Polym Int* 65(9):1046–1053. <https://doi.org/10.1002/pi.5150>
 38. Motaung TE, Liganiso LZ (2018) Critical review on agro-waste cellulose applications for biopolymers. *Int J Plast Technol* 22(2):185–216. <https://doi.org/10.1007/s12588-018-9219-6>
 39. Bhattacharyya A, Pramanik A, Maji SK, Haldar S, Mukhopadhyay UK, Mukherjee J (2012) Utilization of vinasse for production of poly-3-(hydroxybutyrate-co-hydroxyvalerate) by *Haloferax mediterranei*. *AMB Express* 2(1):34
 40. Wang K, Yin J, Shen D, Li N (2014) Anaerobic digestion of food waste for volatile fatty acids (VFAs) production with different types of inoculum: effect of pH. *Bioresour Technol* 161:395–401. <https://doi.org/10.1016/j.biortech.2014.03.088>
 41. Purser BJ, Thai SM, Fritz T, Esteves SR, Dinsdale RM, Guwy AJ (2014) An improved titration model reducing over estimation of total volatile fatty acids in anaerobic digestion of energy crop, animal slurry and food waste. *Water Res* 61:162–170. <https://doi.org/10.1016/j.watres.2014.05.020>
 42. Esteban-Gutiérrez M, García-Aguirre J, Irizar I, Aymerich E (2018) From sewage sludge and agri-food waste to VFA: Individual acid production potential and up-scaling. *Waste Manag* 77:203–212. <https://doi.org/10.1016/j.wasman.2018.05.027>
 43. American Public Health Association (1998) *Water Environment Federation, Standard methods for the examination of water and wastewater*. Stand Methods 541
 44. Jayakumar A, Prabhu K, Shah L, Radha P (2020) Biologically and environmentally benign approach for PHB-silver nanocomposite synthesis and its characterization. *Polym Test* 81:106197. <https://doi.org/10.1016/j.polymertesting.2019.106197>
 45. Das S, Majumder A, Shukla V, Suhazsini P, Radha P (2018) Biosynthesis of poly (3-hydroxybutyrate) from cheese whey by *Bacillus megaterium* NCIM 5472. *J Polym Environ* 26(11):4176–4187. <https://doi.org/10.1007/s10924-018-1288-2>
 46. Li A, Ha Y, Wang F, Li W, Li Q (2012) Determination of thermally induced trans-fatty acids in soybean oil by attenuated total reflectance fourier transform infrared spectroscopy and gas chromatography analysis. *J Agric Food Chem* 60(42):10709–10713. <https://doi.org/10.1021/jf3033599>
 47. Rambabu N, Panthapulakkal S, Sain M, Dalai AK (2016) Production of nanocellulose fibers from pinecone biomass: evaluation and optimization of chemical and mechanical treatment conditions on mechanical properties of nanocellulose films. *Ind Crop Prod* 83:746–754. <https://doi.org/10.1016/j.indcrop.2015.11.083>
 48. Mahardika M, Abrial H, Kasim A, Arief S, Asrofi M (2018) Production of nanocellulose from pineapple leaf fibers via high-shear homogenization and ultrasonication. *Fibers* 6(2):28. <https://doi.org/10.3390/fib6020028>
 49. Ashori A, Jonoobi M, Ayrilmis N, Shahreki A, Fashapoyeh MA (2019) Preparation and characterization of polyhydroxybutyrate-co-valerate (PHBV) as green composites using nano reinforcements. *Int J Biol Macromol* 136:1119–1124. <https://doi.org/10.1016/j.ijbiomac.2019.06.181>
 50. Mohapatra S, Samantaray DP, Samantaray SM, Mishra BB, Das S, Majumdar S, Pradhan SK, Rath SN, Rath CC, Akthar J, Achary KG (2016) Structural and thermal characterization of PHAs produced by *Lysinibacillus* sp through submerged fermentation process. *Int J Biol Macromol* 93:1161–1167. <https://doi.org/10.1016/j.ijbiomac.2016.09.077>
 51. Liu C, Li B, Du H, Lv D, Zhang Y, Yu G, Mu X, Peng H (2016) Properties of nanocellulose isolated from corncob residue using sulfuric acid, formic acid, oxidative and mechanical methods. *Carbohydr Polym* 151:716–724. <https://doi.org/10.1016/j.carbpol.2016.06.025>
 52. Segal L, Creely JJ, Martin AE, Conrad CM (1959) An empirical method for estimating the degree of crystallinity of native cellulose using the X-ray diffractometer. *Text Res J* 29:786–794. <https://doi.org/10.1177/004051755902901003>
 53. Boufi S, Chaker A (2016) Easy production of cellulose nanofibrils from corn stalk by a conventional high speed blender. *Ind Crop Prod* 93:39–47. <https://doi.org/10.1016/j.indcrop.2016.05.030>
 54. Manikandan NA, Pakshirajan K, Pugazhenth G (2020) Preparation and characterization of environmentally safe and highly biodegradable microbial polyhydroxybutyrate (PHB) based graphene nanocomposites for potential food packaging applications. *Int J Biol Macromol*. <https://doi.org/10.1016/j.ijbiomac.2020.03.084>
 55. Fukushima K, Tabuani D, Abbate C, Arena M, Ferreri L (2010) Effect of sepiolite on the biodegradation of poly (lactic acid) and polycaprolactone. *Polym Degrad Stabil* 95(10):2049–2056. <https://doi.org/10.1016/j.polymdegradstab.2010.07.004>
 56. Nagamani P, Chaitanya K, Mahmood SK (2015) Production and characterization of polymer from *Bacillus* OU73T from in-expensive carbon sources. *Int J Curr Microbiol Appl Sci* 4(7):833–840
 57. Moorkoth D, Nampoothiri KM (2016) Production and characterization of poly (3-hydroxy butyrate-co-3 hydroxyvalerate)(PHBV) by a novel halotolerant mangrove isolate. *Bioresour Technol* 201:253–260. <https://doi.org/10.1016/j.biortech.2015.11.046>
 58. Israni N, Venkatachalam P, Gajaraj B, Varalakshmi KN, Shivakumar S (2020) Whey valorization for sustainable polyhydroxyalkanoate production by *Bacillus megaterium*: production, characterization and in vitro biocompatibility evaluation. *J Environ Manag* 255:109884. <https://doi.org/10.1016/j.jenvman.2019.109884>
 59. Silvério HA, Neto WP, Dantas NO, Pasquini D (2013) Extraction and characterization of cellulose nanocrystals from corncob for application as reinforcing agent in nanocomposites. *Ind Crop Prod* 44:427–436. <https://doi.org/10.1016/j.indcrop.2012.10.014>
 60. do Lago RC, de Oliveira AL, Dias MC, de Carvalho EE, Tonoli GH, Boas EV (2020) Obtaining cellulosic nanofibrils from oat straw for biocomposite reinforcement: mechanical and barrier properties. *Ind Crop Prod* 148:112264. <https://doi.org/10.1016/j.indcrop.2020.112264>
 61. Cherpinski A, Torres-Giner S, Vartiainen J, Peresin MS, Lahtinen P, Lagaron JM (2018) Improving the water resistance of nanocellulose-based films with polyhydroxyalkanoates processed by the electrospinning coating technique. *Cellulose* 25(2):1291–1307. <https://doi.org/10.1007/s10570-018-1648-z>
 62. Jun D, Guomin Z, Mingzhu P, Leilei Z, Dagang L, Rui Z (2017) Crystallization and mechanical properties of reinforced PHBV composites using melt compounding: effect of CNCs and CNFs. *Carbohydr Polym* 168:255–262. <https://doi.org/10.1016/j.carbpol.2017.03.076>
 63. Zhou YM, Fu SY, Zheng LM, Zhan HY (2012) Effect of nanocellulose isolation techniques on the formation of reinforced poly (vinyl alcohol) nanocomposite films. *Express Polym Lett*. <https://doi.org/10.3144/expresspolymlett.2012.85>

64. Ahankari SS, Mohanty AK, Misra M (2011) Mechanical behaviour of agro-residue reinforced poly (3-hydroxybutyrate-co-3-hydroxyvalerate), (PHBV) green composites: a comparison with traditional polypropylene composites. *Compos Sci Technol* 71(5):653–657. <https://doi.org/10.1016/j.compscitech.2011.01.007>
65. Zhao X, Ji K, Kurt K, Cornish K, Vodovotz Y (2019) Optimal mechanical properties of biodegradable natural rubber-toughened PHBV bioplastics intended for food packaging applications. *Food Pack Shelf* 21:100348. <https://doi.org/10.1016/j.fpsl.2019.100348>
66. Hassaini L, Kaci M, Touati N, Pillin I, Kervoelen A, Bruzard S (2017) Valorization of olive husk flour as a filler for biocomposites based on poly (3-hydroxybutyrate-co-3-hydroxyvalerate): Effects of silane treatment. *Polym Test* 59:430–440. <https://doi.org/10.1016/j.polymertesting.2017.03.004>
67. Wei L, McDonald AG, Stark NM (2015) Grafting of bacterial polyhydroxybutyrate (PHB) onto cellulose via in situ reactive extrusion with dicumyl peroxide. *Biomacromol* 16(3):1040–1049. <https://doi.org/10.1021/acs.biomac.5b00049>
68. Deepa B, Abraham E, Cordeiro N, Mozetic M, Mathew AP, Oksman K, Faria M, Thomas S, Pothan LA (2015) Utilization of various lignocellulosic biomass for the production of nanocellulose: a comparative study. *Cellulose* 22(2):1075–1090. <https://doi.org/10.1007/s10570-015-0554-x>
69. Benini KC, Ornaghi Júnior HL, Bianchi O, de Magalhães WF, Henriques FF, Windmoller D, Voorwald HJ, Cioffi MO (2019) Novel biodegradable composites based on PHBV: Effect of nanocellulose incorporation on the non-isothermal crystallization kinetic and structural parameters. *Polym Compos* 40(8):3156–3165. <https://doi.org/10.1002/pc.25164>
70. Wei L, Stark NM, McDonald AG (2015) Interfacial improvements in biocomposites based on poly (3-hydroxybutyrate) and poly (3-hydroxybutyrate-co-3-hydroxyvalerate) bioplastics reinforced and grafted with α -cellulose fibers. *Green Chem* 17(10):4800–4814. <https://doi.org/10.1039/C5GC01568E>
71. Panaitescu DM, Nicolae CA, Gabor AR, Trusca R (2020) Thermal and mechanical properties of poly (3-hydroxybutyrate) reinforced with cellulose fibers from wood waste. *Ind Crop Prod* 145:112071. <https://doi.org/10.1016/j.indcrop.2019.112071>
72. Yu HY, Qin ZY, Liu YN, Chen L, Liu N, Zhou Z (2012) Simultaneous improvement of mechanical properties and thermal stability of bacterial polyester by cellulose nanocrystals. *Carbohydr Polym* 89(3):971–978. <https://doi.org/10.1016/j.carbpol.2012.04.053>
73. Makaremi M, Pasbakhsh P, Cavallaro G, Lazzara G, Aw YK, Lee SM, Milioto S (2017) Effect of morphology and size of halloysite nanotubes on functional pectin bionanocomposites for food packaging applications. *ACS Appl Mater Interface* 9(20):17476–17488. <https://doi.org/10.1021/acsami.7b04297>

Publisher's Note Springer Nature remains neutral with regard to jurisdictional claims in published maps and institutional affiliations.